

Plasma density temporal evolution in a high-power microwave pulse compressor switch

L. BEILIN, A. SHLAPAKOVSKI, M. DONSKOY, T. QUELLER and YA. E. KRASIK

Physics Department, Technion - Haifa 32000, Israel

received 16 December 2014; accepted 6 January 2015

published online 28 January 2015

PACS 52.80.Pi – High-frequency and RF discharges

PACS 52.70.Kz – Optical (ultraviolet, visible, infrared) measurements

PACS 52.75.Kq – Plasma switches (*e.g.*, spark gaps)

Abstract – Time-resolved optical-emission spectroscopy measurements are used to evaluate plasma density in an interference switch during the extraction of a nanosecond output pulse from a high-power microwave compressor. The compressor represents a resonant cavity connected to an H-plane waveguide tee with a shorted side arm filled with helium at a pressure of $2 \cdot 10^5$ Pa; the plasma discharge in the tee side arm is triggered by a Surelite laser. A nanosecond-scale dynamics of the plasma density is obtained by analyzing the shape of the helium spectral lines. The analysis of the experimental data evidences a correlation between the rise time of the plasma density and the peak power of the microwave output pulse. Numerical simulations of the microwave energy release from the cavity with the appearance of the plasma yield results in good agreement with the measured output pulse peak power and waveform.



Copyright © EPLA, 2015

Introduction. – Microwave plasma discharges have been widely investigated for many years because of the interesting basic phenomena involved in microwave breakdown in gases and the development of various microwave plasma generators [1]. There is, however, a subject that is insufficiently studied, namely, the dynamics of the plasma formation at the initial —nanosecond time-scale— stage of the high-pressure discharge in a resonant cavity and its interrelation with the process of microwave energy release from the cavity that goes out of resonance during the plasma generation. This subject directly concerns the operation of high-gain high-power resonant microwave compressors, in which the characteristic time of energy release is about the round-trip time for a traveling electromagnetic wave along the cavity —usually several nanoseconds [2]. Thus, the plasma build-up in the switches employed in these compressors should be in the nanosecond time range, providing a density on the one hand sufficient for efficient extraction of the energy stored in the cavity and on the other not too large to minimize Ohmic losses.

Recently, the first experiments on fast-frame (2 ns) imaging of light emission from the plasma in the switch of the resonant microwave compressor with laser triggering were conducted [3]. The images obtained showed that

the plasma appears as filaments having a diameter < 1 mm and expanding with velocity $\sim 5 \cdot 10^7$ cm/s along the RF electric field. Based on the results obtained, the plasma density was estimated as $\leq 10^{17}$ cm $^{-3}$. Imaging, however, is rather inappropriate for quantitative evaluation of the plasma density and its temporal dynamics. A more suitable non-disturbing method is time-resolved optical-emission spectroscopy, the implementation of which is described in detail, for instance, in [4].

In this work, spectroscopic measurements are applied to characterize the plasma density evolution in the H-plane waveguide tee-based interference switch of a resonant compressor with laser triggering. We employed helium as the gas filling the system, since helium is appropriate for spectroscopy measurements, *i.e.*, it is an atomic gas free of chemical reactions for which verified data that allow one to derive the plasma density from the line-shape analysis are available [5,6]. Because of the low breakdown threshold of helium, the RF electric field built up before the discharge triggering was limited (15–20 kV/cm at a pressure of $2 \cdot 10^5$ Pa), so that the compressor output power was moderate. One can, nevertheless, assume that findings of the present study apply also to gases withstanding fields of hundreds of kV/cm built up in compressors capable of hundreds of megawatt output power.

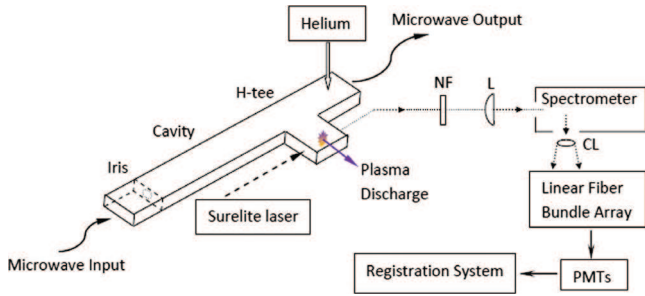


Fig. 1: (Color online) Schematic of experimental setup.

Experimental setup and results. – The experimental setup is shown in fig. 1. The microwave compressor was the same as that described in detail in [3], providing about the same gain (output-to-input power ratio). The compressor operated at a frequency of 2766.9 MHz; its output pulses had the same typical waveform as presented in [3] (~ 8 ns full width at half maximum (FWHM)), differing from those of [3] by a moderate peak power level because of employing helium and, respectively, reduced input power. The Surelite laser beam ($\lambda = 532$ nm, ~ 50 mJ, ~ 7 ns FWHM) was used to initiate the plasma discharge in the tee side arm at the quarter guide wavelength from the shorting plane. The laser beam was directed through the waveguide perpendicular to the RF electric field and blocked by the notch filter NF placed at the opposite side of the tee side arm (see fig. 1). The light emitted from the discharge was focused by the lens L onto the entrance slit of the Spex 750M spectrometer. At the exit of the spectrometer, the cylindrical lens CL formed the image at the entrance of the linear fiber bundle array. The latter consists of 9 bundles with 91 fibers in each. The light from each bundle carrying a certain spectral interval was transported to a Hamamatsu H10721-01 photo-multiplier tube (PMT). Signals from 9 PMTs were recorded by TDS 784A oscilloscopes (1 GHz, 4 GS/s) allowing us to record spectral lines with time resolution of 0.25 ns. The spectral resolution of the optical setup was varied by changing the positions of the CL and fiber array and measured using Oriel spectral calibration lamps.

Temporal evolution of two sufficiently intensive He I spectral lines, triplet $2s-3p$ (3888.65 Å) and triplet $2p-4d$ (4471.5 Å), was studied. For the 3888.65 Å line, FWHMs were used to determine the dynamics of the plasma density; in the case of the 4471.5 Å line, the ratios of intensities of forbidden ($2p-4f$) and allowed components were used. The spectral resolution was ≈ 0.3 Å/fiber-bundle in the case of 3888.65 Å line and ≈ 0.45 Å/fiber-bundle for the 4471.5 Å line.

Typical examples of normalized spectrally resolved light emission from the plasma obtained in the cases of low (~ 90 kW) and high (~ 330 kW) peak output microwave power are shown in fig. 2. Here, the time $t = 0$ corresponds to the moment when the compressor output pulse reaches a maximal power. One can see that the temporal behavior

of light emission strongly correlates with the measured power of the microwave output pulse. Qualitatively similar behavior was obtained for all light emission pulses corresponding to a low (≤ 100 kW) and high (> 200 kW) peak output power. Namely, the rise in intensity of light emission is much steeper in the case of high-power output than in the low-power microwave output. In addition, the time delay between the moment when the laser beam enters the switch and the appearance of the light emission was found to be significantly shorter for the case of higher power of the microwave output pulse. The difference in these delays was 30 ± 15 ns; the jitter is the sum of ± 6 ns jitter for the high-power and ± 9 ns for the low-power case, calculated from series of 31 and 39 pulses, respectively.

Here, let us note that the time jitter for the appearance of microwave output with respect to the moment when the laser beam enters the switch was the same as for the optical signals. Therefore, the representation of time with respect to the microwave peak is convenient for eliminating rather frequently observed irregularity in the intensity of light emission (caused by photon statistics) by summing normalized intensities from 10–20 pulses yielding a close value of output power. This approach for the analysis was used when the said irregularity did not allow reasonable results to be achieved by the analysis of data obtained in single pulses.

In fig. 3, one can see typical examples of spectral lines obtained from the analysis of optical signals and examples of the plasma density evolution in time derived from obtained spectra for both He I 3888.65 Å and 4471.5 Å lines. In the case of the 3888.65 Å line, the Voigt fit was applied to determine the Lorentzian FWHM, taking into account the instrumental broadening of the setup (0.64 Å) measured preliminarily using Oriel calibration lamp. The obtained Lorentzian FWHM is mainly the sum of the Stark and van der Waals broadening (estimates of the Doppler and resonance line broadening allow one to ignore them). Thus, by applying the same analysis as described in [4] and using the tabulated data in [5], the temporal evolution of the plasma electron density was obtained. In fig. 3(c), the calculated electron density dynamics is presented for the three single pulses with different microwave output power. Here, the time is counted with respect to the moment of the laser beam's entrance into the tee side arm. It should be noted that, since the calculated electron density is proportional to the Stark broadening and the experimental error of the line width measurement (~ 0.05 Å) is fixed, the error in the density evaluation increases significantly as the Lorentzian FWHM obtained approaches the value of the van der Waals broadening (0.158 Å), *i.e.*, for lower plasma densities. Nevertheless, one can draw a certain conclusion from the curves regarding the density temporal evolution, namely, for a higher compressor output power, a steeper rise in the plasma density was obtained. One can see also that the plasma density increases approaching $6 \cdot 10^{16}$ cm $^{-3}$ and the plasma appears earlier in time as the microwave output power increases.

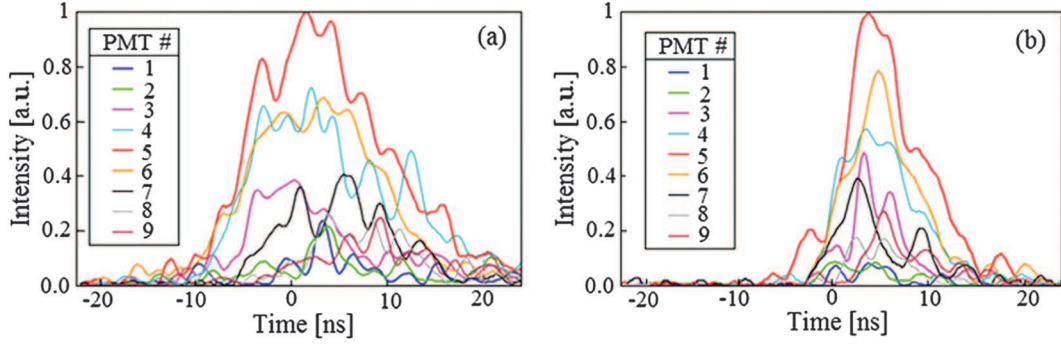


Fig. 2: (Color online) Light intensity registered by 9 PMTs *vs.* time in two pulses differing in the level of the compressor output power: ~ 90 kW (a) and ~ 330 kW (b). Time is with respect to the peak of microwave output signal. The wavelength delivered to PMTs descends with the PMT number; the PMT No. 5 corresponds to 3888.65 \AA .

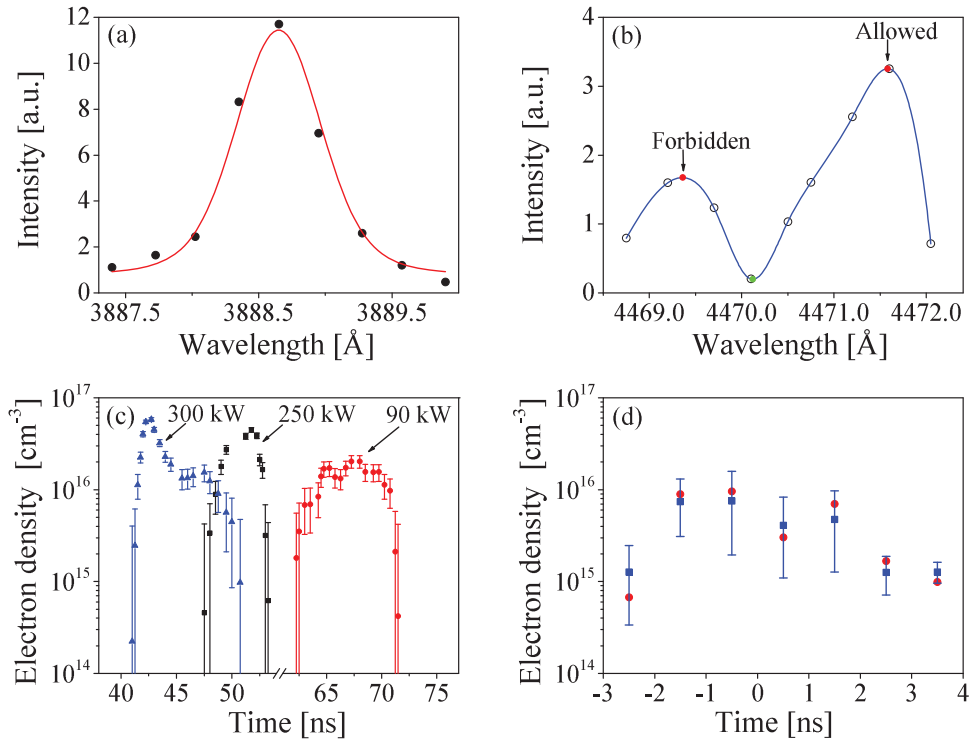


Fig. 3: (Color online) Typical shapes of the spectral lines (top) and examples of the plasma density evaluation (bottom) for the 3888.65 \AA ((a), (c)) and 4471.5 \AA ((b), (d)) lines. In (c), the density is derived from the data obtained in single pulses differing by the microwave peak output power: ~ 90 kW (red circles), ~ 250 kW (black squares), ~ 300 kW (blue triangles); time is with respect to the moment of the laser beam entrance into the tee side arm. In (d), red circles correspond to the density derived from the data obtained by summing normalized intensities of optical signals over 12 pulses with close output power (≥ 150 kW), blue squares represent the mean density obtained from the intensities of these 12 optical pulses; time is with respect to the peak of output power.

In the case of the 4471.5 \AA spectral line, for the analysis the spline approximation was applied to the points obtained from 9 PMT output signals at a fixed moment of time to determine the peaks in intensities corresponding to the allowed and forbidden components. The ratio of intensities was used to calculate the plasma electron density according to the formula (20) in [6]. As the 4471.5 \AA spectral line is less intensive than the 3888.65 \AA one, the

recorded optical signals are more irregular, so that the abovementioned approach of summing data from single pulses with time counting from the peak of microwave output signal was used. In addition, the influence of irregularity was suppressed by building spectra averaged over the 1 ns time interval. The calculated plasma density dynamics presented in fig. 3(d) shows a similar evolution in time as that obtained for the 3888.65 \AA line,

and the plasma density level is in satisfactory agreement as well.

Numerical simulations. – Correlation between the plasma density dynamics and the compressor output power was found also in the numerical simulations of the microwave energy release from the compressor. The simulations were carried out with the 3-D version of the fully electromagnetic particle-in-cell (PIC) code MAGIC [7] using the gas conductivity model of plasma embedded in the code. In this model, the conductivity is determined by the electron and ion densities and mobilities depending on the electric field and pressure; the densities evolve according to the equations accounting for the avalanche, recombination, and external ionization rate. The simulations started from the preset RF fields obtained in the simulations of the compressor charging without plasma. The initial plasma density corresponding to the cosmic background, 10^4 cm^{-3} , was set in the cavity, and the initial population of macroparticles (electrons) with charge density of 10^{-11} C/cm^3 and randomly distributed velocities was set around the RF electric field antinode in the tee side arm within the 1.2-mm-side cubic volume. The rate of external ionization Q_e was calculated from PIC dynamics and ionization cross-sections, $Q_e = \frac{qN}{e\Delta V} \sum_i v_i \sigma_{ion}(v_i)$, where q and v_i are the charge and velocity of a macroparticle, respectively, σ_{ion} is the cross-section, N is the neutral gas number density, and ΔV is the cell volume of the computational grid. The avalanche rate α as a function of the RF electric field module E was set using the empirical formula for the Townsend coefficient for inert gases [1] yielding $\alpha = CE \exp(-DE^{-1/2})$, where the coefficients C and D were calculated from the table data for helium [1] for the pressure being $2 \cdot 10^5 \text{ Pa}$.

In fig. 4, the results of the simulations are shown for the cases of low (the preset electric field maximal amplitude in the tee side arm was $\sim 16.6 \text{ kV/cm}$) and high (the preset field maximum was $\sim 22.3 \text{ kV/cm}$) microwave output power. The recorded microwave output pulses corresponding to the PMT signals, which were used to plot the plasma density *vs.* time curves in fig. 3(c) ($\sim 300 \text{ kW}$ and $\sim 90 \text{ kW}$ peak power), are also plotted in fig. 4. One can see that the simulated waveform of the output pulse very well agrees with that obtained in the experiment for the high-power case; for the low-power case, the agreement can be considered satisfactory. The delay time needed for the simulated output pulse to be formed is significantly longer for the low-power case; the difference in this delay time is very close to that registered in the corresponding pulses. The rise time and the pulse duration are longer, and the efficiency of power extraction are lower for the low-power case, as in the experiments. The dense plasma evolves as a filament extending along the RF electric field direction, as was observed in [3]; the transverse size of the filament is determined by the initial electron population volume. The moment of time when the plasma density in the location of the initial population reaches

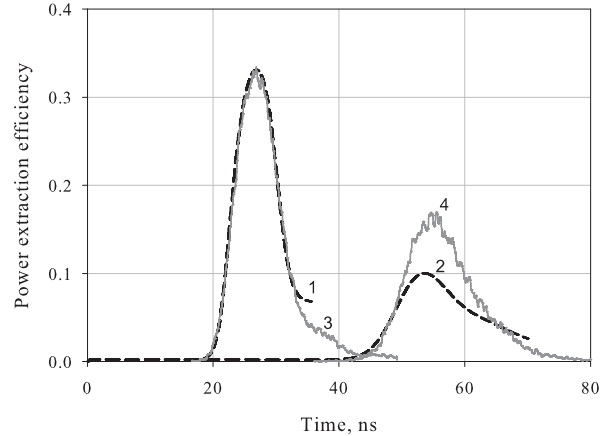


Fig. 4: Comparison of the simulated microwave output power pulses (dashed curves) with those obtained in the experiments (solid curves). For each curve, the power is normalized to the power of the traveling-wave component of the RF field in the compressor cavity — preset in the simulations or measured in the experiments (maximal power achieved by the beginning of output pulse extraction). 1, 3: high-power case; 2, 4: low-power case.

its maximum approximately coincides with the moment of the microwave peak, as observed in experiments.

The agreement with the experiment is much better for the high-power case than for the low-power one because the triggering event is modeled by setting the same density in the initial electron population volume in both cases. Meanwhile, initial electrons are generated by the combined action of the laser and RF electric field, and their density is lower for a lower RF field, *i.e.*, for the low-power case, in the experiment it is lower than was set in the simulation. As a result, the time needed for the RF energy release to begin is slightly longer in the experiment (see fig. 4, curve 2 and 4), leading to a higher plasma density in the filament that is formed by the electron avalanche outside the initial cubic volume. Therefore, in the experiment, the output power is higher than the simulated one.

Conclusions. – To summarize, spectroscopic measurements of the emitted light were carried out to obtain the nanosecond dynamics of the plasma density in the interference switch of the S-band resonant microwave compressor with laser triggering. The measured evolution of the density in time evidently correlates with the peak power of the compressor output pulse and efficiency of the stored microwave energy extraction. With increasing microwave output, the plasma appears earlier in time after the laser beam enters the system, the plasma density rises more steeply, and it reaches higher values.

This work was supported in part by the BSF grant No. 2012038 and under the framework of the KAMEA Program of the Ministry of Immigrant Absorption and the Council for Higher Education, State of Israel. The authors

are thankful to Dr A. SAYAPIN for the assistance and discussions.

REFERENCES

- [1] RAIZER YURI P., *Gas Discharge Physics* (Springer-Verlag, Berlin, Heidelberg) 1991.
- [2] BENFORD J., SWEGLE J. A. and SCHAMLOGLU E., *High Power Microwaves*, 2nd edition (Taylor & Francis, New York, London) 2007.
- [3] BEILIN L., SHLAPAKOVSKI A., DONSKOY M., HADAS Y., DAI U. and KRASIK YA. E., *IEEE Trans. Plasma Sci.*, **42** (2014) 1346.
- [4] YATOM S., STAMBULCHIK E., VEKSELMAN V. and KRASIK YA. E., *Phys. Rev. E*, **88** (2013) 013107.
- [5] GRIEM H. R., *Spectral Line Broadening by Plasmas* (Academic Press, New York) 1974.
- [6] CZERNICHOWSKI A. and CHAPELLE J., *J. Quant. Spectrosc. Radiat. Transfer*, **33** (1985) 427.
- [7] GOPLEN B., LUDEKING L., SMITHE D. and WARREN G., *Comput. Phys. Commun.*, **87** (1995) 54.